REPORT DOCUMENTATION PAGE

Form Approved OMB NO. 0704-0188

1. REPORT DATE (DD-MM-YYYY)	2. REPORT TYPE	3. DATES COVERED (From - To)
18-06-2017	Final Report	19-Mar-2014 - 18-Mar-2017

4. TITLE AND SUBTITLE
Final Report: Redox-Switchable Coordination Catalysis: An Advanced Tool for Catalyst Control and Tailored Polyolefin Synthesis

5a. CONTRACT NUMBER
W911NF-14-1-0138

5b. GRANT NUMBER

5c. PROGRAM ELEMENT NUMBER
611102

6. AUTHORS
Brian K. Long

5d. PROJECT NUMBER

5e. TASK NUMBER

5f. WORK UNIT NUMBER

7. PERFORMING ORGANIZATION NAMES AND ADDRESSES
University of Tennessee at Knoxville
Office of Sponsored Programs
1534 White Avenue
Knoxville, TN 37996 -1529

8. PERFORMING ORGANIZATION REPORT NUMBER

9. SPONSORING/MONITORING AGENCY NAME(S) AND ADDRESS (ES)
U.S. Army Research Office
P.O. Box 12211
Research Triangle Park, NC 27709-2211

10. SPONSOR/MONITOR'S ACRONYM(S)
ARO

11. SPONSOR/MONITOR'S REPORT NUMBER(S)
64823-CH-YIP.7

12. DISTRIBUTION AVAILIBILITY STATEMENT
Approved for Public Release; Distribution Unlimited

13. SUPPLEMENTARY NOTES
The views, opinions and/or findings contained in this report are those of the author(s) and should not contrued as an official Department of the Army position, policy or decision, unless so designated by other documentation.

14. ABSTRACT
The growing demand for polyolefins with tailored physical and mechanical properties has guaranteed that the development of innovative polymerization catalysts will persist at the frontier of scientific research. Though early olefin polymerization catalysts were ill-defined, heterogeneous mixtures containing multiple dissimilar active sites, the introduction of well-defined, homogeneous, single-site catalysts has since revolutionized the field of polyolefin research. Single-site catalysts have tremendous flexibility in ligand design, which has presented new opportunities for mechanistic understanding, catalyst control, and polyolefin synthesis that are impossible using heterogeneous

15. SUBJECT TERMS
Catalysis, Redox Switchable, Polyolefin, Microstructure, Copolymerization, Ethylene, Lactide

16. SECURITY CLASSIFICATION OF:			17. LIMITATION OF ABSTRACT	15. NUMBER OF PAGES	19a. NAME OF RESPONSIBLE PERSON
a. REPORT	b. ABSTRACT	c. THIS PAGE			Brian Long
UU	UU	UU	UU		19b. TELEPHONE NUMBER 865-974-6534

RPPR

as of 12-Oct-2017

Agency Code:

Proposal Number: **Agreement Number:**

Organization:
Address: , ,
Country:
DUNS Number: EIN:
Report Date: Date Received:
for Period Beginning and Ending
Title:
Begin Performance Period: **End Performance Period:**
Report Term: -
Submitted By: Email:
Phone:

Distribution Statement: -

STEM Degrees: **STEM Participants:**

Major Goals:

Accomplishments:

Training Opportunities:

Results Dissemination:

Plans Next Period:

Honors and Awards:

Protocol Activity Status:

Technology Transfer:

Redox-Switchable Coordination Catalysis: An Advanced Tool for Catalyst Control and Tailored Polyolefin Synthesis

Principle Investigator: Brian K. Long
Organization: University of Tennessee
Department of Chemistry
1420 Circle Dr.
Knoxville, TN 37996

ARO Proposal Number: 64823-CH-YIP
Agreement Number: W911NF-14-1-0138

Report Author: Brian K. Long
Report Type: Final Progress Report (FPR)
Reporting Period: March 19, 2014 – March 18, 2017
Final Report Date: June 18, 2017

1. Forward (optional – not included)
2. Table of Contents (not included, report < 10 pages)
3. List of Appendices (not applicable)

4. Statement of the Problem Studied

The growing demand for polyolefins with tailored physical and mechanical properties has guaranteed that the development of innovative polymerization catalysts will persist at the frontier of scientific research. Though early olefin polymerization catalysts were ill-defined, heterogeneous mixtures containing multiple dissimilar active sites,[1,2] the introduction of well-defined, homogeneous, single-site catalysts has since revolutionized the field of polyolefin research. Single-site catalysts have tremendous flexibility in ligand design, which has presented new opportunities for mechanistic understanding, catalyst control, and polyolefin synthesis that are impossible using heterogeneous catalyst systems.[1,3-7] These benefits have ensured that single-site catalysts remain an extremely attractive target in industry and academia alike, though many fundamental questions remain to be answered.

To advance fundamental understanding within olefin polymerization catalysts, specifically the role that ligand electronics play on catalytic performance, we proposed to develop redox-switchable polymerization catalysis (RSPC) as a cutting-edge tool for catalyst control and tailored polymer synthesis. RSPC's ability to modulate catalytic behavior via simple changes in ligand oxidation state will bring innovative opportunities for enhanced catalyst design and polymer synthesis. To accomplish this overall goal, we have focused our efforts on the following two main projects:

- **Project 1** – Develop redox-active olefin polymerization catalysts,[8] and explore the effect that ligand oxidation state has on their catalytic behavior, polyolefin topology, and comonomer incorporation.
- **Project 2** – Develop redox-active lactide polymerization catalysts and explore the effect that ligand oxidation state has on their catalytic behavior.

5. Summary of Most Important Results

Project 1 – *Redox-Switchable Olefin Polymerization Catalyst:*

Our initial investigations focused on the redox capabilities of a simple α-diimine-based complex (**1**) in an attempt to establish redox-switchable olefin polymerization catalysis (RSOPC) in the field of olefin polymerization. This well-defined complex utilizes an organic-based redox-active site, which is an acenaphthenequinone-derived α-diimine ligand (Figure 1), in place of traditionally used metal-based redox-active centers that have plagued all previous attempts at RSOPC.

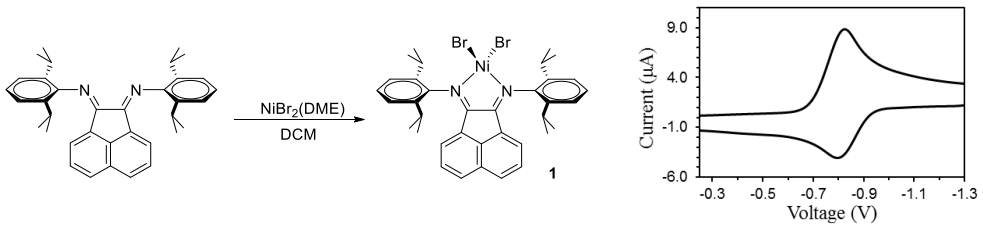

Figure 1. Synthesis of α-diimine-based catalysts $\mathbf{1_{ox}}$ and its redox behavior by CV.

Ethylene Homopolymerization: Ethylene polymerization trials were conducted following established procedures using PMAO-IP as an activator (Table 1, entries 3−7). Polymerizations requiring the reduced catalyst were conducted by adding ≤1 equiv of cobaltocene into the polymerization reactor containing catalyst **1** and toluene prior to injection of PMAO-IP activator. Despite achieving remarkably similar yields, molecular weights, and dispersities, ^{1}H NMR analysis revealed a highly reproducible correlation between the amount of cobaltocene added to the polymerization reactor and the microstructure of the resultant PE. For example, polymerizations conducted using catalyst **1** produced PE with ~30% more branches per 1000 total carbons (114 ± 1.9 branches/1000 C's) than polymerizations conducted using catalyst **1** and 1 equiv of added cobaltocene (88 ± 2.8 branches/1000 C's) (Figure 2). Furthermore, if the amount of added cobaltocene was varied from 0 to 1 equiv (relative to catalyst 1), an almost linear relationship with branching density was observed (Figure 2 left).

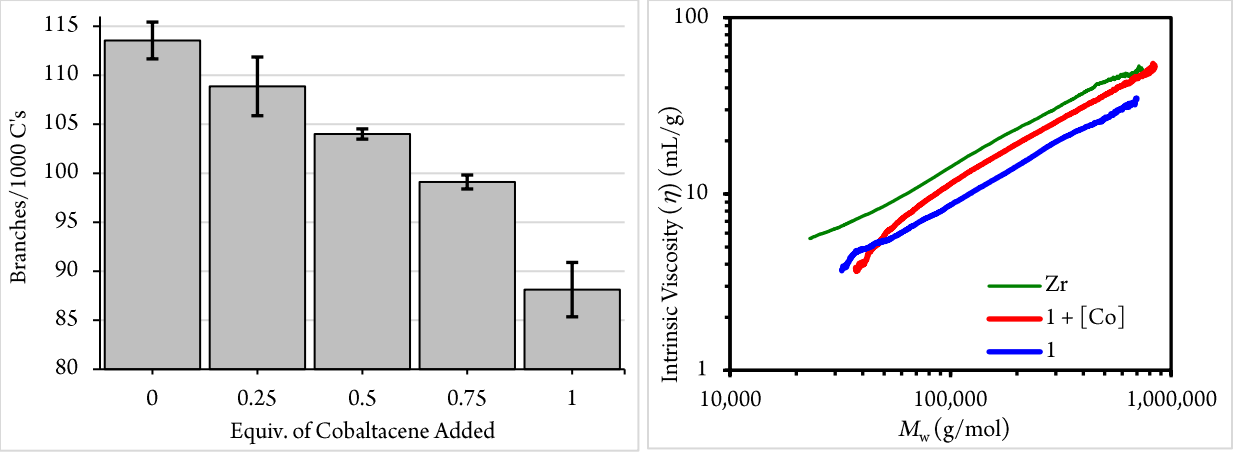

Figure 2. *Left:* Plot of branches per 1000 total C's vs equivalents of cobaltocene added relative to catalyst 1. *Right:* Log-log plot of intrinsic viscosity (η) vs M_w for PE samples polymerized at 20 °C.

This differentiation in branching was also confirmed via size exclusion chromatography (SEC) and their Mark-Houwink log-log plots of [η] vs M_w (Figure 2). Quantitative ^{13}C NMR analysis revealed that as the equivalents of added cobaltocene were increased, the polymers produced displayed a greater percentage of methyl branches (54.9% → 62.8%) and branches that were six carbons and longer (9.2% → 10.4%). In contrast, a corresponding decrease in the percentage of ethyl, propyl, and butyl branches was also observed as a function of increasing equivalents of reductant. Perhaps the most intriguing result was the virtual elimination of sec-butyl branching from polymer samples synthesized using catalyst **1** reduced by 1 equiv of cobaltocene.[9] The observed reduction in sec-butyl branching from 5.3% to 0.9% strongly indicates that catalyst **1**'s propensity to chain-walk past a tertiary centers is dramatically hindered when reduced catalyst **1** is used. ***This virtual elimination of all branch-on-branch PE structure signifies a small, yet very real change in PE branching topology as a result of ligand oxidation state, which is the first ever reported.***

Olefin Copolymerization – To expand the scope of this redox-active polymerization methodology, redox-active catalyst **1** was examined for the polymerization of higher α-olefins and the copolymerization of α-olefins with ethylene. Propylene polymerizations employing catalyst **1** and $CoCp_2$ (1.0 equiv) were found to display an approximately five-fold reduction in turnover frequency (TOF) (2,627 vs 452) at room temperature. In similarity, 1-hexene polymerizations in the presence of 1.0 equiv of $CoCp_2$ displayed a 3-4 times reduction in TOF (1,916 vs 644) (Figure 3). Despite the reduced rate of 1-hexene conversion for catalyst **1** in the presence of 1.0 equiv of $CoCp_2$, the yields and molecular weights of the resultant poly(1-hexene) were found to steadily increase throughout the 6 h polymerization period reaching molecular weights up to 158 kg/mol at full monomer conversion with moderate molecular weight distributions ($Đ$ = 1.21 → 1.99) (Figure 3).

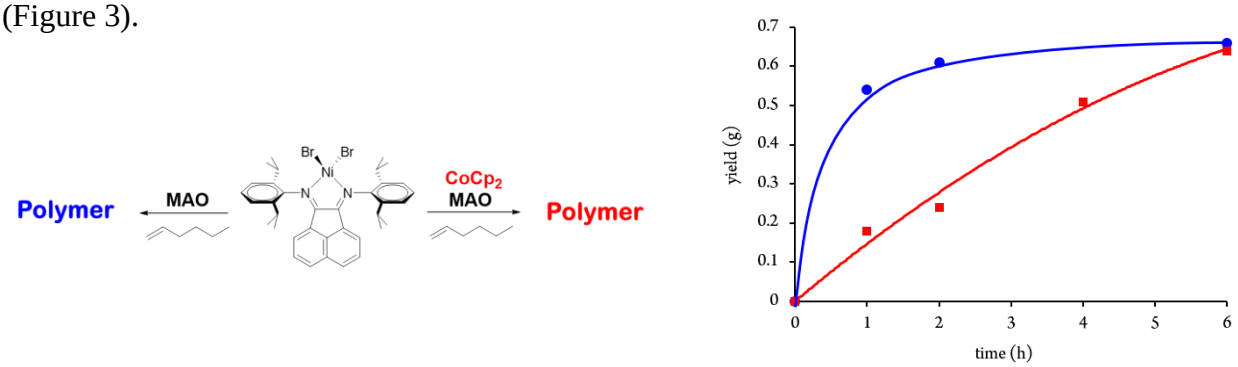

Figure 3. Plot of yield vs. time for the polymerization of 1-hexene using catalyst **1** in the presence of $CoCp_2$ (1 equiv) (red squares) and absence of $CoCp_2$ (blue circles).

Encouraged by this differentiation in conversion rate for higher α-olefin homopolymerizations and capitalizing on the fact that catalyst **1**'s displayed no dependence in TOF for ethylene polymerizations,[12] we chose to evaluate the copolymerization of ethylene and 1-hexene. The results of these copolymerizations are detailed in Table 1 in which both polymer yield (3.4 g → 2.1 g) and molecular weight (M_n = 179 kg/mol → 110 kg/mol) were found to decrease as a function of added $CoCp_2$. Branching analysis of the copolymer samples via ^{1}H NMR spectroscopy revealed a 22% decrease in branching content as a function of added reductant (108 → 85 branches/1000 total carbons) (Table 1). Analysis of each copolymer's branching identity by quantitative ^{13}C NMR spectroscopy revealed that between ~21-31 % of all branches were butyls, strongly indicating that

1-hexene was likely incorporated to a significant degree in all cases. In comparison, ethylene homopolymerizations in the presence or absence of added reductant were found to only produce ~6.7-9.0 % butyl branches.

Table 1. Ethylene/1-Hexene Copolymerization Data[a]

entry	$CoCp_2$ (μmol)	yield (g)	M_n[b] (kg/mol)	M_w/M_n[b]	B[c,d]
1	0	3.4 (±0.3)	179	1.47	108 (±0.6)
2	5	2.5 (±0.2)	167	1.60	94 (±2.9)
3	10	2.1 (±0.3)	110	1.71	85 (±2.5)

[a]Polymerization conditions: [**1**] = 10.0 μmol, 15 psi ethylene, 5 mL of 1-hexene, 148 mL of toluene, 2 mL of dichloromethane, 30 min, and 92 equiv of MAO. [b]Determined using triple detection gel permeation chromatography at 140 °C in 1,2,4-trichlorobenzene. [c]Branches per 1000 total carbons determined via 1H NMR. [d]Average of multiple trials.

To confirm and quantitate the consumption of 1-hexene during these copolymerizations, the polymerization solutions were analyzed via gas chromatography (GC) immediately after quenching. As expected, 1-hexene consumption decreased sharply as the amount of added $CoCp_2$ was increased from 0.0 to 1.0 equiv relative to catalyst **1**. More specifically, the percentage of 1-hexene consumed in each polymerization was 13.0 %, 7.9 %, and 4.5% per gram of polymer produced when 0.0, 0.5, and 1.0 equiv of $CoCp_2$ was added, respectively (Figure 4). This result not only confirmed that the significant number of butyl branches present in these copolymers is a direct result of 1-hexene incorporation, but also emphasizes that the amount of 1-hexene being incorporated is strongly dependent on the presence and amount of $CoCp_2$ added. ***This finding represents the first report of controlling comonomer composition during a one-pot copolymerization using a redox event.***

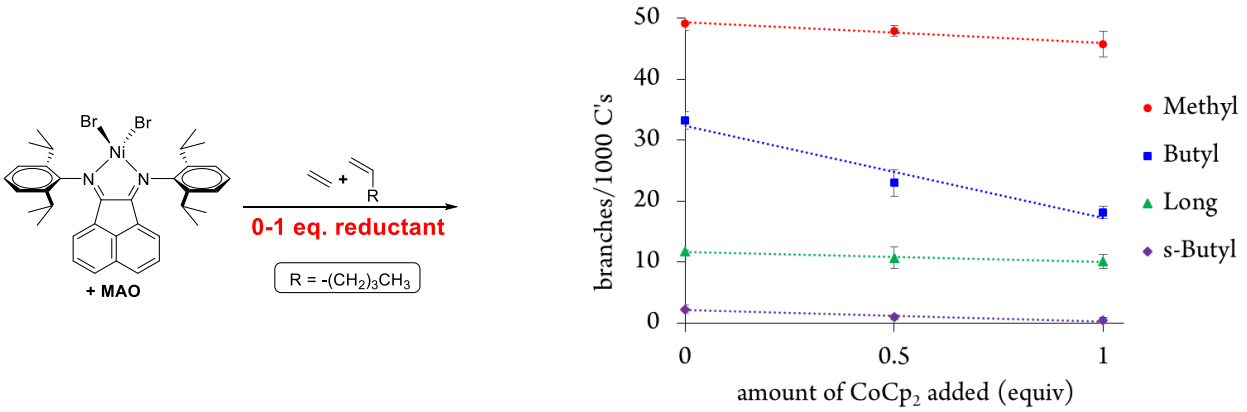

Figure 4. Plot of methyl (red circles), butyl (blue squares), long (green triangles), and sec-butyl (purple diamonds) branches/1000 C's for copolymers produced using **1** as a function of added reductant ($CoCp_2$).

Accessing Multiple Polyethylene Grades from a single Catalyst – In an effort to demonstrate the utility of this redox switching behavior, we designed and synthesized a second generation catalyst, complex **3** (Figure 5). We predicted that the very electron donating ferrocenyl substituents should donate electron density to the active metal site, and might also open up the possibility to access more than one oxidation site. Furthermore, cyclic voltammetry confirmed that two redox potentials could be observed which could be ascribed to the ferrocenyl moieties and acenapthyl backbone of the catalyst structure, respectively.

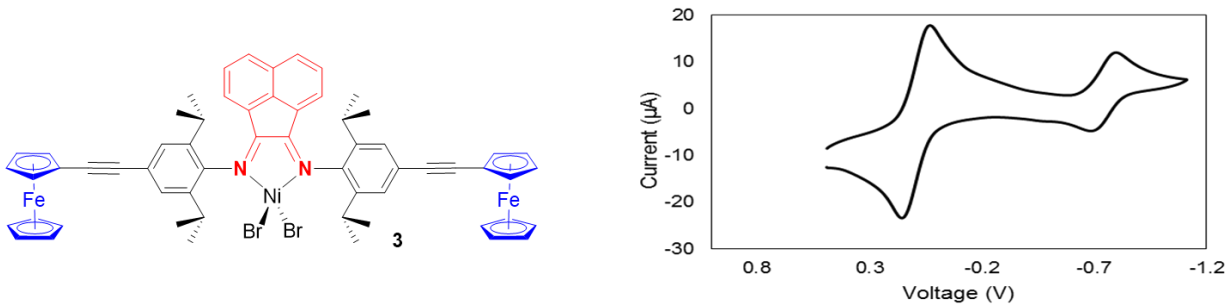

Figure 5. Catalyst **3** and is CV trace.

Catalyst **3** was used to polymerize ethylene as described for catalyst **1** above. It was found that when polymerizing in the presence of 1 equiv of added reductant that high molecular weight PE could be obtained possessing only 9 branches per 1000 carbons. Measurement of the polymers density via Archmides principle revealed that it was medium-density PE (MDPE) (Figure 6). In contrast, ethylene polymerizations using catalyst 3 and no added reductant were found to produce PE with 40 branches per 1000 carbons, which corresponded to very-low-density PE (VLDPE). ***This remarkable differentiation represents the first ever report of changing a polymer grade via simple addition or removal of an electron to the active catalytic species.***

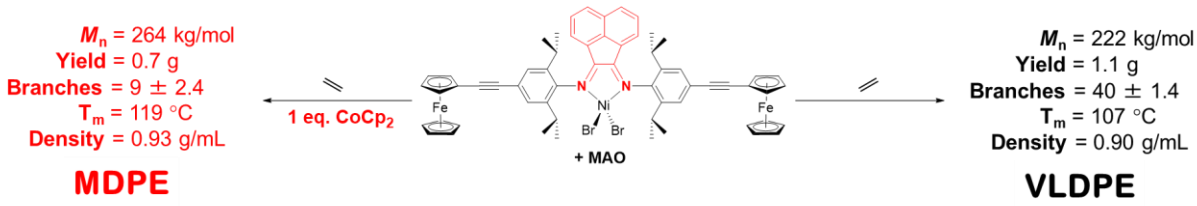

Figure 6. Ethylene polymerization using catalyst **3** with or without added reductant.

Lastly, attempts to oxidize the ferrocenyl moieties have led to minimal results. This is believed to be due to the known incompatibility of oxidized ferrocenyl moieties in the presence of reducing alkyl aluminum species, such as the trimethyl aluminum found in our methaluminoxane activator. Attempts to avoid this are currently ongoing.

Computational/Experimental Investigations into Catalyst 1's Structure and Behavior – To better understand the origins of catalyst **1**'s behavior as a function of added reductant we needed to understand the electronic structure of reduced catalyst **1**. Previous studies suggest that reduced catalyst **1** could potentially exist as any one of many possibilities that can include: 1) a radical anionic ligand form in which the added electron is delocalized over the ligands bisimidoethane bridge, 2) a form in which the transition-metal is reduced from Ni(II) to Ni(I), or 3) a structure in which the catalyst complex has been reduced by more than one electron.[14-19] To probe which of these scenarios might contribute to the polymerization behavior observed, we utilized electron paramagnetic resonance (EPR) spectroscopy, magnetic susceptibility, and UV-Vis spectroscopy. EPR experiments indicated that upon reduction of catalyst **1** with 1 equivalent of cobaltacene, a formal reduction of Ni(II) to Ni(I) was observed yielding a *g*-value of 2.342. Addition of trimethyl aluminum (5 equivalents) to this Ni(I) complex resulted in rapid metal-to-ligand electron transfer from the Ni(I) center to the ligand itself, thereby creating a ligand-based, carbon-centered radical

(g = 2.002). This proposed reaction scheme was supported by magnetic susceptibility and UV-Vis spectroscopic measurements.[14]

To shed further light onto this matter, we have engaged the help of Prof. Sharani Roy (UT) to pursue this structure and mechanistic study via computational methods. Though those studies are not yet complete, we have calculated a number of structures and transition states that all agree with the hypotheses made in the previous sections. Furthermore they strongly support that the structure of the reduced complex is indeed one in which the coordinating ligand is radical anionic in nature and that the propagating metal species is in fact a neutral Ni^{II} species (Figure 7).

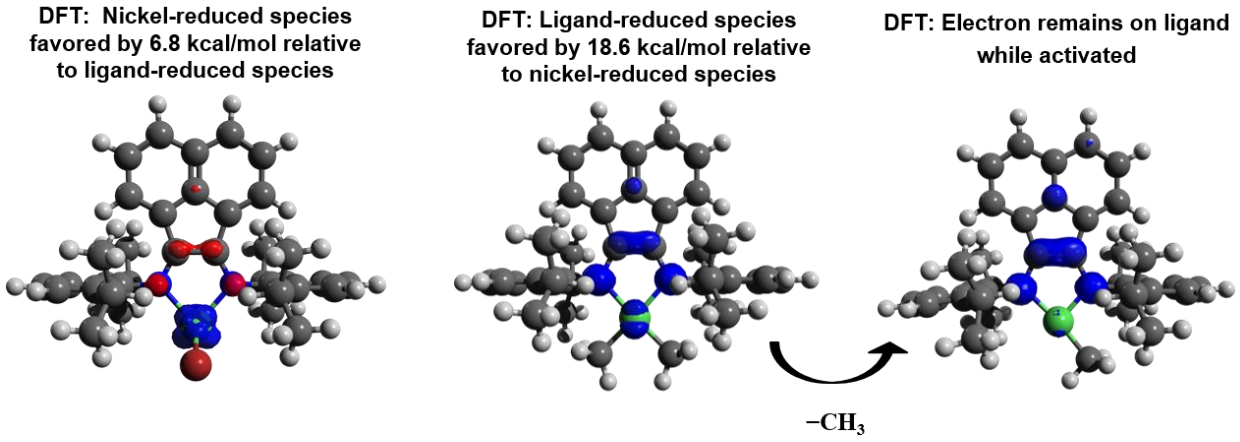

Figure 7. Calculated structures of reduced complex **1** using DFT theory.

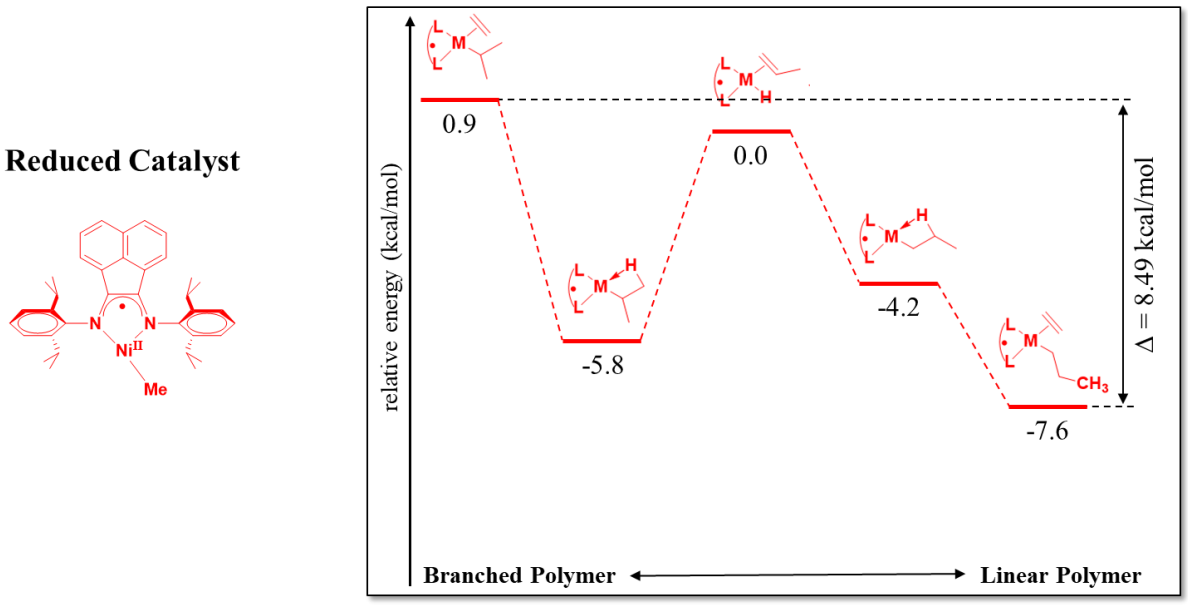

Figure 8. Computational examination of branching for the reduced catalyst **1**.

To explain the observed reduction in PE branch content observed when using the reduced catalyst **1**, further calculations were performed at the triple zeta level in which the relative free energies (ΔG) of each species along the mechanistic path that is required to install a PE branch were analyzed. AS can be seen in Figure 8, a dramatic increase in ΔG (+8.49 kcal/mol relative to linear ethylene polymerization) is observed when a branch point is created. In comparison, native catalyst 1 only displays a +0.89 kcal/mol difference between its branched insertion relative to linear ethylene polymerization. We believe it is this difference in energies that directly accounts for the decrease in branching observed for ethylene polymerizations using catalyst **1**. Lastly, similar calculations are currently being performed to explain the observed differences in 1-hexene incorporation.

Project 2 – ***Redox-Switchable Lactide Polymerization Catalyst:***

We successfully synthesized catalyst **2**, but quickly found that it performed poorly for the polymerization of olefins. Catalyst **2** did however prove to be a very interesting candidate for the polymerization of lactide, and is a closely related analogue of a catalyst previously reported by Gibson and co-workers.[7] To gain fundamental understanding into the effect that ferrocenyl group proximity (to the active metal site) has on the redox-switchable polymerization of lactide, we investigated the catalytic differences between catalyst **4** and those previously reported (Figure 9).

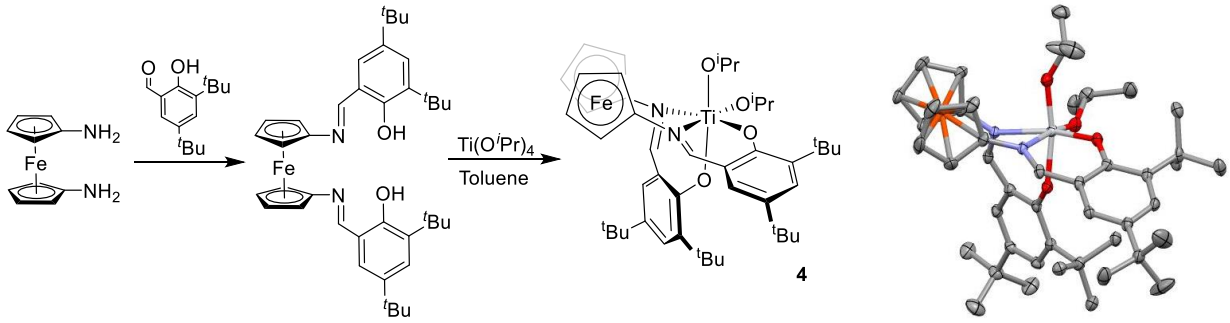

Figure 9. Synthesis and X-ray crystal structure of redox-active catalyst **4**.

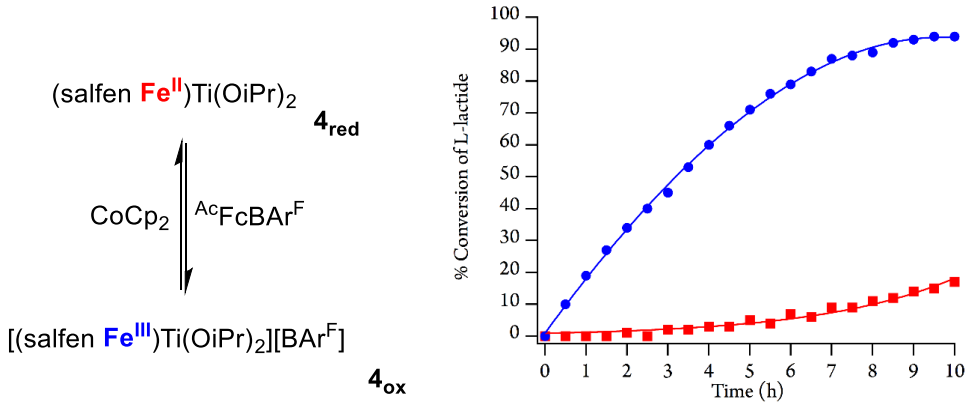

Figure 10. Plot of polymerization conversion versus time for the polymerization of L-lactide (100 equiv, 1 M) in C_6D_6 at 90 °C using catalyst $\mathbf{4_{red}}$ (red squares) or $\mathbf{4_{ox}}$ (blue circles) (NOTE: the oxidation of catalyst $\mathbf{4_{red}} \rightarrow \mathbf{4_{ox}}$ was performed prior to monomer addition).

Catalyst **4** was adopt an unusual *β-cis* conformation by NMR and X-ray crystallographic analysis. When the catalytic activity of catalyst was investigated for the ring-opening polymerization of L-lactide, it was discovered that the oxidized catalyst polymerized at a much greater rate than its reduced analogue (Figure 10). This observation was in stark contrast to the report by Gibson in which they described that their oxidized catalyst polymerized lactide at a much slower rate than its reduced analogue. This unusual behavior was attributed to the unusual *β-cis* conformation of this catalyst.

To study the redox-switchability of catalyst **4**, *in situ* switching experiments were performed using acetylferrocenium borate as an oxidant and cobaltocene as a reductant. The results of this experiment are shown in Figure 11. Unexpectedly, the catalytic behavior of catalyst **4** proved to be very complex in which upon initial oxidation the catalyst rapidly began to consume lactide monomer, but subsided after reaching ~4-6% conversion (Figure 11, time period B). Even more interestingly, all subsequent re-reductions and re-oxidations yielded catalytic behavior that was opposite (Figure 11, time periods C, D, and E) to what was originally observed in Figure 5.

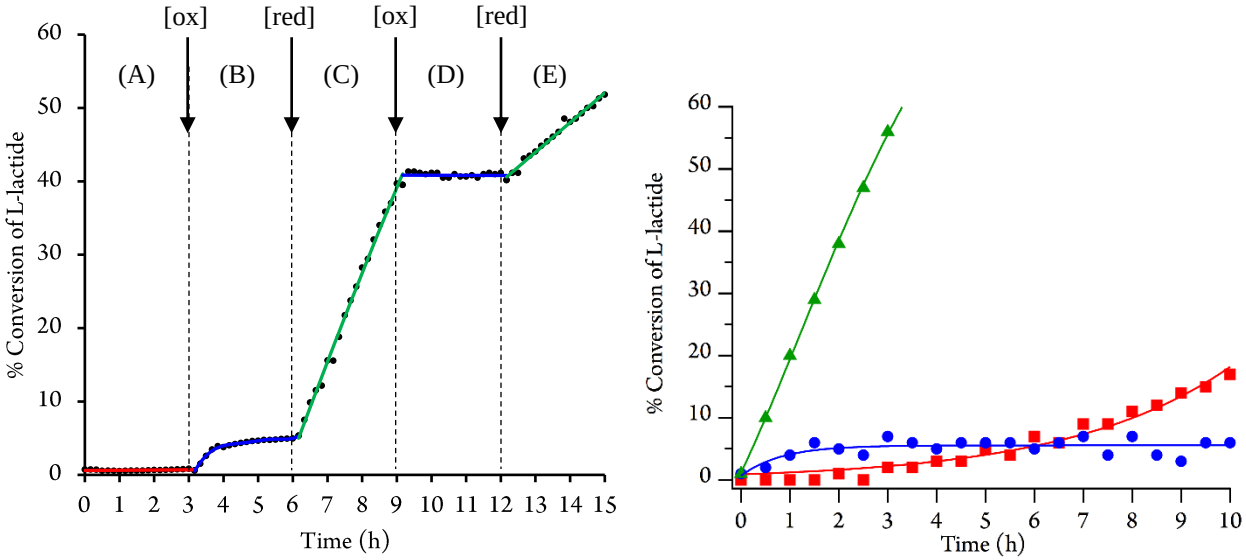

Figure 11. *Left:* Plot of conversion versus time for the polymerization of L-lactide in C_6D_6 at 90 °C with in situ redox-switching, starting with catalyst 4. *Right:* Plot of conversion versus time for the polymerization of L-lactide (100 equiv, 1 M) in C_6D_6 at 90 °C using catalyst 4_{red} (red squares), oxidized catalyst 4_{ox} (blue circles), and re-reduced catalyst 4_{red} (green triangles).

Efforts then turned to understanding the physical reason for this change in catalytic behavior, which did not appear to be directly linked to the redox-activity of the ferrocenyl moiety. Further investigations revealed that when catalyst **4** was oxidized in the presence of excess monomer, a change in catalyst geometry was observed (evidenced by ^{1}H NMR and cyclic voltammetry) and was likely the cause for the *in situ* change in catalytic behavior. This was further proven when the experiments described in Figure 9 were reproduced, but in which the catalyst was oxidized in the presence of excess monomer (Figure 11, right). As predicted, similar behavior was observed in which the oxidized catalyst rapidly reached ~4-6% monomer conversion, but then remained constant after that point. This result exactly mimicked the *in situ* behavior observed in Figure 10,

time period B. ***We believe that this evidence supports the first example of a catalyst that not only undergoes redox-switching, but that undergoes a change in ligand geometry in situ.***

Summary for all Projects:

Through this funded ARO-YIP effort we have:

1. Established that redox switchable catalysis is a viable tool for polyolefin synthesis.
2. Demonstrated clear differentiation between reduced and oxidized states of an active olefin polymerization catalyst with regards to ethylene homopolymerizations and the influence that redox-active catalysts have with respect to polyolefin branching content and topology.
3. Determined that reduced catalytic catalyst **1** polymerizes higher α-olefins at a much slower rate than its non-reduced analogue which can be harnessed to control polyolefin comonomer incorporation percentages and thus its polymer microstructure.
4. Examined the structure of our catalyst using a battery of both experimental and computational techniques to better understand the complex chemistry underlying.
5. Proven that ferrocenyl proximity in redox active lactide catalysts play a crucial role in reactivity.
6. Proven that ligand geometry may be fluxional during these lactide polymerizations and must be carefully accounted for.

We want to thank the ARO for their generous support of this work and we feel strongly that these projects push the current boundaries of catalyst development knowledge and polymer microstructural control. Without the ARO, none of this science would have been possible.

6. Bibliography:

(1) Coates, G. W. *Chem. Rev.* **2000**, *100*, 1223-1252.
(2) Hlatky, G. G. *Chem. Rev.* **2000**, *100*, 1347-1376.
(3) Gibson, V. C.; Spitzmesser, S. K. *Chem. Rev.* **2003**, *103*, 283-315.
(4) Zohuri, G. H.; Albahily, K.; Schwerdtfeger, E. D.; Miller, S. A. *Polymer Science: A Comprehensive Reference*; Elsevier, 2012; Vol. 3.
(5) Alt, H. G.; Köppl, A. *Chem. Rev.* **2000**, *100*, 1205-1222.
(6) Chen, E. Y. X.; Marks, T. J. *Chem. Rev.* **2000**, *100*, 1391-1434.
(7) Ittel, S. D.; Johnson, L. K.; Brookhart, M. *Chem. Rev.* **2000**, *100*, 1169-1203.
(8) Lyaskovskyy, V.; de Bruin, B. *ACS Catalysis* **2012**, *2*, 270-279.
(9) Cotts, P. M.; Guan, Z.; McCord, E.; McLain, S. *Macromolecules* **2000**, *33*, 6945-6952.
(10) Galland, G. B.; de Souza, R. F.; Mauler, R. S.; Nunes, F. F. *Macromolecules* **1999**, *32*, 1620-1625.
(11) Azoulay, J. D.; Bazan, G. C.; Galland, G. B. *Macromolecules* **2010**, *43*, 2794-2800.
(12) Anderson, W. C.; Rhinehart, J. L.; Tennyson, A. G.; Long, B. K. *J. Am. Chem. Soc.* **2016**, *138*, 774-777.
(13) Galland, G. B.; Quijada, R.; Rojas, R.; Bazan, G.; Komon, Z. J. A. *Macromolecules* **2002**, *35*, 339-345.
(14) Fedushkin, Igor L.; Skatova, Alexandra A.; Chudakova, Valentina A.; Cherkasov, Vladimir K.; Fukin, Georgy K.; Lopatin, Mikhail A. *European Journal of Inorganic Chemistry* **2004**, *2004*, 388-393.

(15) Khusniyarov, M. M.; Harms, K.; Burghaus, O.; Sundermeyer, J. *European Journal of Inorganic Chemistry* **2006**, *2006*, 2985-2996.
(16) van Asselt, R.; Elsevier, C. J.; Amatore, C.; Jutand, A. *Organometallics* **1997**, *16*, 317-328.
(17) Cole, B. E.; Wolbach, J. P.; Dougherty, W. G.; Piro, N. A.; Kassel, W. S.; Graves, C. R. *Inorg. Chem.* **2014**, *53*, 3899-3906.
(18) Fedushkin, I. L.; Skatova, A. A.; Chudakova, V. A.; Fukin, G. K. *Angew. Chem. Int. Ed.* **2003**, *42*, 3294-3298.
(19) Fedushkin, I. L.; Skatova, A. A.; Lukoyanov, A. N.; Khvoinova, N. M.; Piskunov, A. V.; Nikipelov, A. S.; Fukin, G. K.; Lysenko, K. A.; Irran, E.; Schumann, H. *Dalton Trans* **2009**, 4689-4694.